Scaling of the linear response function from zero-field-cooled and thermoremanent magnetization in phase-ordering kinetics

Federico Corberi,* Eugenio Lippiello,† and Marco Zannetti‡
Istituto Nazionale di Fisica della Materia, Unità di Salerno and Dipartimento di Fisica "E. Caianiello," Università di Salerno, 84081 Baronissi (Salerno), Italy

(Received 13 May 2003; published 28 October 2003)

In this paper we investigate the relation between the scaling properties of the linear response function $R(t,s)$, of the thermoremanent magnetization (TRM) and of the zero-field-cooled (ZFC) magnetization in the context of phase-ordering kinetics. We explain why the retrieval of the scaling properties of $R(t,s)$ from those of TRM and ZFC magnetization is not trivial. Preasymptotic contributions generate a long crossover in TRM, while ZFC magnetization is affected by a dangerous irrelevant variable. Lack of understanding of both these points has generated some confusion in the literature. The full picture relating the exponents of all the quantities involved is explicitly illustrated in the framework of the large-N model. Following this scheme, an assessment of the present status of numerical simulations for the Ising model can be made. We reach the conclusion that on the basis of the data available up to now, statements on the scaling properties of $R(t,s)$ can be made from ZFC magnetization but not from TRM. From ZFC data for the Ising model with $d=2,3,4$ we confirm the previously found linear dependence on dimensionality of the exponent a entering $R(t,s) \sim s^{-(1+a)} f(t/s)$. We also find evidence that a recently derived form of the scaling function $f(x)$, using local scale invariance arguments [M. Henkel, M. Pleimling, C. Godrèche, and J. M. Luck, Phys. Rev. Lett. **87**, 265701 (2001)], does not hold for the Ising model.

DOI: 10.1103/PhysRevE.68.046131 PACS number(s): 05.70.Ln, 75.40.Gb, 05.40.−a

I. INTRODUCTION

The behavior of systems out of equilibrium is a subject of wide current interest [1]. Most of the attention is focused on glassy or disordered systems. Nonetheless, many of the interesting features of slow relaxation, such as aging, can be studied also in the simpler context of a phase-ordering process. This is the dynamical process which takes place, for instance, when a ferromagnet is suddenly cooled from above to below the critical point. Then, ordered regions grow by coarsening. The process is slow, i.e., the typical size of these regions increases with the power law $L(t) \sim t^{1/z}$, where z is the dynamic exponent. For dynamics with nonconserved order parameter (NCOP), as it will be considered in this paper, $z=2$ independent of dimensionality. In an infinite system equilibrium is never reached. Phase ordering has been studied for a long time now [2]. However, despite its relative simplicity when compared to the complexity of glassy behavior, there still remains lack of consensus and considerable confusion about the properties of the off equilibrium response function. This paper is devoted to clarify the issue. This is not a problem of minor importance, given that phase ordering is regarded as a paradigmatic example of out of equilibrium behavior.

For definiteness, let us think of an Ising ferromagnet with Hamiltonian

$$\mathcal{H}[\sigma] = -J \sum_{\langle i,j \rangle} \sigma_i \sigma_j , \tag{1}$$

initially prepared at very high temperature and quenched at the time $t=0$ to a final temperature $T<T_C$. In a process of this type the initial magnetization is zero and remains zero at all times $\langle \sigma_i(t) \rangle = 0$ for $t \geqslant 0$. Quantities of interest are [3] the autocorrelation function

$$C(t,s,t_0,t_{sc},t_{eq}) = \langle \sigma_i(t) \sigma_i(s) \rangle, \tag{2}$$

where $t \geqslant s \geqslant 0$ are two times after the quench and the linear (auto)response function

$$R(t,s,t_0,t_{sc},t_{eq}) = \left. \frac{\partial \langle \sigma_i(t) \rangle}{\partial h_i(s)} \right|_{h=0}, \tag{3}$$

where $h_i(s)$ is the external field conjugated to the order parameter. Traditionally, in phase-ordering studies most of the attention has been devoted to the correlation function [2], while the response function has remained in the background.

In addition to the two observation times t and s, in Eqs. (1) and (2) we have explicitly indicated also a dependence on the following characteristic times.

$t_0 \sim \Lambda^{-z}$. This is a microscopic time related, through the dynamic exponent z, to such a microscopic length as the lattice spacing or the inverse momentum cutoff Λ^{-1}.

t_{sc}. The process of phase ordering is characterized by dynamical scaling in the asymptotic time region (or late stage). The characteristic time t_{sc} separates the preasymptotic from the asymptotic regime, i.e., it gives a measure of how much time is needed after the quench for scaling to set in.

t_{eq}. After the formation of domains of ordered regions, equilibrium is rapidly reached in the interior of domains. The characteristic time needed to establish this local equilibrium is the same as the equilibration time in the pure ordered

*Email address: corberi@na.infn.it
†Email address: lippiello@sa.infn.it
‡Email address: zannetti@na.infn.it

phases. It is given by $t_{eq} \sim \xi^z$, where ξ is the equilibrium correlation length in the pure phases at the final temperature T and z is the dynamic exponent introduced above.

The correlation and response functions can always be written as the sum of two contributions [3]:

$$C(t,s,t_0,t_{sc},t_{eq}) = C_{st}(t-s,t_0,t_{eq}) + C_{ag}(t,s,t_0,t_{sc}), \tag{4}$$

$$R(t,s,t_0,t_{sc},t_{eq}) = R_{st}(t-s,t_0,t_{eq}) + R_{ag}(t,s,t_0,t_{sc}), \tag{5}$$

where the stationary contributions are what one has in equilibrium in the pure phases. Therefore, the usual fluctuation-dissipation theorem is satisfied

$$R_{st}(t-s,t_0,t_{eq}) = \frac{1}{T}\frac{\partial C_{st}(t-s,t_0,t_{eq})}{\partial s}. \tag{6}$$

The rest, the aging contributions $C_{ag}(t,s,t_0,t_{sc})$ and $R_{ag}(t,s,t_0,t_{sc})$, are what is left over due to the existence of slow out of equilibrium degrees of freedom. The above split is useful for s sufficiently large, i.e., for

$$s \gg t_{eq} \tag{7}$$

in order to have well separated time scales for equilibrium and nonequilibrium behaviors and for

$$s \gg t_{sc} \tag{8}$$

in order for $C_{ag}(t,s,t_0,t_{sc})$ and $R_{ag}(t,s,t_0,t_{sc})$ to exhibit scaling behavior.

In connection with the aging contributions there are two basic questions.

(i) How do $C_{ag}(t,s,t_0,t_{sc})$ and $R_{ag}(t,s,t_0,t_{sc})$ scale in the late stage?

(ii) What is the relation between $C_{ag}(t,s,t_0,t_{sc})$ and $R_{ag}(t,s,t_0,t_{sc})$, if any?

The second question belongs to the general area of the out of equilibrium generalization of the fluctuation-dissipation theorem [4]. This is a problem not as trivial as it is believed to be for phase-ordering systems [5,6], with interesting implications on the connection between statics and dynamics [7]. In this paper we concentrate on the first question which is preliminary to the second one.

Assuming that s is large enough for Eqs. (7) and (8) to be satisfied and dropping t_{sc}, the scaling form of $C_{ag}(t,s,t_0)$ is given by

$$C_{ag}(t,s,t_0) \sim s^{-b} g(t/s, t_0/s). \tag{9}$$

It is well known [2] that $b=0$. Furthermore, for $s \gg t_0$ one can set $y=0$ in $g(x,y)$ and it is also well known that for $x \gg 1$ one has $g(x,0)=g(x) \sim x^{-\lambda/z}$, where λ is the Fisher-Huse exponent. Information about $R_{ag}(t,s,t_0)$, instead, is scanty. Writing the scaling relation analogous to Eq. (9) in the form

$$R_{ag}(t,s,t_0) = s^{-(1+a)} f(t/s, t_0/s) \tag{10}$$

both a and $f(x,y)$ are much less known than b and $g(x,y)$. Despite considerable efforts, no consensus has been reached as of yet on the value of a. The situation for the scaling function $f(x,y)$ is not much better. Recently, Henkel, Pleimling, Godrèche, and Luck (HPGL) [8], using local scale invariance [9], have derived an explicit form of the scaling function which is supposed to be of general validity. However, under close scrutiny this form appears neither to be obeyed in those cases where an exact solution is available, nor to fit numerical data for Ising systems, as will be shown in Sec. III.

There is more than one reason for such an unsatisfactory state of affairs. The first one is due to a qualitative analysis [10] of the relation between the response function and the density of defects. A naive use of this argument leads to the conclusion that a is independent of dimensionality, e.g., for scalar systems $a=1/z$. In this form, due to its simplicity, this argument has become deeply rooted in the literature [7,11–13], despite the accumulation of exact [14–16], approximated [5,13], and numerical results [5,17,18] incompatible with it. As we shall see, $R_{ag}(t,s,t_0)$ is trivial in the sense that it is proportional to the defect density only in the short time regime, but in no case this implies that a is independent of dimensionality. Another reason is that in simulations $R_{ag}(t,s,t_0)$ is too noisy to work with and, in order to deal with more manageable quantities, one must resort to the integrated response functions (IRFs). The price for this is that reconstructing the scaling properties of $R_{ag}(t,s,t_0)$ from those of an IRF is not as simple as it might look at first sight [18]. This will be the main theme of the paper.

We will show that, through the combined use of exact results and numerical simulations, definite conclusions can be reached for the exponent a by analyzing in detail what actually goes on in the different methods employed to evaluate it. For what concerns the scaling function $f(x,y)$, instead, our understanding of the problem remains incomplete.

The paper is organized as follows. In Sec. II we review existing information about $R_{ag}(t,s,t_0)$, make general considerations on the scaling function, and comment on the HPGL theory. In Sec. III we analyze the problem of retrieving the properties of $R_{ag}(t,s,t_0)$ from those of an IRF concentrating on the zero-field-cooled magnetization. Section IV is devoted to the same problem from the side of the thermoremanent magnetization. In Sec. V we use the solution of the large-N model as an explicit illustration clarifying what goes on when different IRF are employed to obtain information on $R_{ag}(t,s,t_0)$. Concluding remarks are made in Sec. VI.

II. WHAT IS KNOWN ABOUT R_{ag}

This paper is devoted to the study of the exponent a and the scaling function $f(x,y)$ entering Eq. (10). We first summarize what is known from exact and approximate analytical results providing direct access to $R_{ag}(t,s,t_0)$. We, then, make general considerations on $f(x,y)$ and some remarks on the HPGL form for it.

Ising model $d=1$. In the exact analytical computation of the response function [14,15] in the $d=1$ kinetic Ising model

with Glauber dynamics, after taking $s \gg t_{sc}$ and neglecting t_0/s, one finds

$$R_{ag}(t,s) \sim s^{-1}(t/s-1)^{-1/2} \tag{11}$$

from which follows

$$a=0 \tag{12}$$

and

$$f(x,0) \sim (x-1)^{-1/2}. \tag{13}$$

Furthermore, the correlation function is given by [19,20]

$$C(t,s)=\frac{2}{\pi}\arcsin\sqrt{\frac{2}{1+t/s}}, \tag{14}$$

which gives $C(t,s) \sim (t/s)^{-1/2}$ for $t/s \gg 1$. Hence, recalling $z=2$, one has $\lambda=1$ and Eq. (13) can be rewritten as

$$f(x,0) \sim \frac{x^{a+1/2-\lambda/z}}{(x-1)^{a+1/2}}. \tag{15}$$

It should be mentioned that $a=0$ has been found numerically also in the case of the kinetic Ising chain with Kawasaki dynamics [21].

Large-N model. Solving analytically the large-N model we have found [16] (see also Sec. V) $R_{ag}(t,s,t_0)$ of form (10) with

$$a=(d-2)/2 \tag{16}$$

and

$$f(x,y) \sim \frac{x^{a+1-\lambda/z}-1}{(x-1+y)^{a+1}}, \tag{17}$$

where d is arbitrary and $\lambda=d/2$. Notice that $a=0$ for $d=2$.

Gaussian auxiliary field (GAF) approximation. Berthier, Barrat, and Kurchan [13] have calculated analytically an IRF using a GAF approximation based on the Ohta-Jasnow-Kawasaki method [2]. From their computation it is easy to extract $R_{ag}(t,s,t_0)$ which is in form (10) with

$$a=(d-1)/2 \tag{18}$$

and

$$f(x,y) \sim \frac{x^{a+1/2-\lambda/z}}{(x-1+y)^{a+1/2}} \tag{19}$$

with $\lambda=d/2$. Their calculation involves a diffusion constant of the form $D=(d-1)/d$ which prevents letting $d \to 1$, so they consider $d \geqslant 2$. We have worked out [5] an alternative GAF approximation, without restriction on dimensionality, which extends Eqs. (18) and (19) to $d \geqslant 1$. Then, we recover $a=0$ for $d=1$ as in the Ising case.

A. General form of $f(x,y)$ and implications for $R_{ag}(t,s,t_0)$

All the above results for $f(x,y)$ are of the form

$$f(x,y) \sim \frac{x^{-\beta}-\epsilon}{(x-1+y)^{\alpha}}, \tag{20}$$

where $\epsilon=0$ if the correlation length in the low-temperature pure phase is finite, like in the $d=1$ Ising model and in the GAF approximation, or $\epsilon=1$ if the low-temperature phase is critical [22] like in the large-N model [16] (see also Sec. V).

We now make the phenomenological assumption that Eq. (20) is valid in general. Then the task becomes that of finding the exponents a, α, and β. For this it is useful to look at the short and long time behaviors.

Short time behavior. Let us rewrite $R_{ag}(t,s,t_0)$ introducing the time difference $\tau=t-s$ in Eq. (20),

$$R_{ag}(t,s,t_0)=s^{\alpha-(1+a)}\left[\frac{(\tau/s+1)^{-\beta}-\epsilon}{(\tau+t_0)^{\alpha}}\right]. \tag{21}$$

Keeping τ fixed and letting s to become large, to lowest order in τ/s we find

$$R_{ag}(t,s,t_0) \sim s^{-\delta}\left[\frac{\tau^{\epsilon}}{(\tau+t_0)^{\alpha}}\right] \tag{22}$$

with

$$\delta=(1+a)-(\alpha-\epsilon) \tag{23}$$

and where ϵ is the same as in Eq. (20). Therefore, from the short time behavior one can extract δ. An important observation is that in the three explicit cases considered above, δ coincides with the exponent entering in the time dependence of the density of defects. At the time s, this is given by

$$L(s)^{-n} \sim s^{-n/z}, \tag{24}$$

where $L(s)$ and z are the domain size and the dynamic exponent introduced above, $n=1$ for $N=1$, $n=2$ for $N>1$, and N is the number of components of the order parameter [2]. One can, then, immediately verify that

$$\delta=n/z. \tag{25}$$

In the $d=1$ Ising model and in the GAF approximation where $\epsilon=0$ and

$$\alpha=a+1/2 \tag{26}$$

from Eq. (23) we get $\delta=1/2$, while in the large-N model with $\epsilon=1$ and

$$\alpha=a+1 \tag{27}$$

we get $\delta=1$.

Long time behavior. In the large time regime $t/s \gg 1$, from Eqs. (10) and (20) follows

$$R_{ag}(t,s,t_0) \sim s^{-(1+a)}(t/s)^{-\lambda_R/z} \tag{28}$$

with

$$\lambda_R/z=\alpha+\beta. \tag{29}$$

Summarizing, the exponents a, α, and β can be obtained, in principle, by making three different measurements on $R_{ag}(t,s,t_0)$: (1) s dependence for fixed t/s gives a [from Eq. (10)]; (2) s dependence for fixed τ gives δ [from Eq. (22)]; and (3) t dependence for fixed s gives λ_R/z [from Eq. (28)]. Before going into this, let us comment on the form of the scaling function derived by HPGL in Ref. [8].

B. Response function from local scale invariance

Without making separation (5) between stationary and aging components and neglecting the dependence on t_0, HPGL assume that the full response function $R(t,s)$ obeys the scaling form

$$R(t,s)\sim s^{-(1+a)}f_{HPGL}(t/s). \tag{30}$$

Then, using local scale invariance arguments they make the prediction that, in general, for phase ordering, one has

$$f_{HPGL}(x)\sim\frac{x^{a+1-\lambda/z}}{(x-1)^{a+1}}, \tag{31}$$

where λ is the Fisher-Huse exponent, provided there are no long range correlations in the initial condition. In support of Eq. (31), they invoke the exact solution of the spherical model [23–25], which is equivalent to the large-N model, and numerical simulations for the Ising model with $d=2$ and $d=3$. We make the following comments.

In the spherical or large-N model Eq. (31) indeed reproduces the full response function. This coincides with the aging contribution (17) for $x\gg1$ but not for $x\simeq1$. This difference will turn out to be important (see Sec. V).

Equation (31) is contained in the general form (20) with $\epsilon=0$, $\beta=\lambda/z-(a+1)$, and $\alpha=a+1$. Inserting into Eq. (23) follows that in all cases one finds the unphysical result $\delta=0$. Furthermore, one should also have $\alpha=a+1$ always, while from the explicit examples considered above this is true only in the large-N case and not in the $d=1$ Ising model or in the GAF approximation.

HPGL theory is supposed to hold also for quenches at T_C. In that case the validity of Eq. (31) has been questioned in the framework of the field theoretic methods for the response function [26].

About the support to Eq. (31) from numerical simulations, we will comment below.

Now, in order to go beyond the explicitly solvable cases, the problem is to determine the exponents a, α, and β in the Ising model with $d>1$. As stated in the Introduction, measurement of $R_{ag}(t,s,t_0)$ is too noisy, so the program outlined in Sec. II A on the basis of Eqs. (22) and (28) requires an unrealistically long computing time. In the following section we discuss how to proceed with the help of IRF.

III. ZERO-FIELD-COOLED MAGNETIZATION

Indirect information on $R_{ag}(t,s,t_0)$ comes from numerical results on IRF. In general, an IRF is defined by

$$\mu(t,t_2,t_1,t_0,t_{sc},t_{eq})=\int_{t_1}^{t_2}dsR(t,s,t_0,t_{sc},t_{eq}) \tag{32}$$

with $t\geqslant t_2\geqslant t_1\geqslant0$ and using Eq. (5) one has

$$\mu(t,t_2,t_1,t_0,t_{sc},t_{eq})=\mu_{st}(t-t_2,t-t_1,t_0,t_{sc},t_{eq})+\mu_{ag}(t,t_2,t_1,t_0,t_{sc}). \tag{33}$$

We will concentrate on the second contribution in the right hand side. The reason for introducing an IRF is that the integration over (t_1,t_2) lowers the noise. However, if one has to resort to an IRF, there is the related problem of retrieving the properties of $R(t,s)$ from it. This is not straightforward. IRFs usually employed are the following.

(1) The thermoremanent magnetization (TRM),

$$\rho(t,t_w,t_0,t_{sc},t_{eq})=\mu(t,t_2=t_w,t_1=0,t_0,t_{sc},t_{eq}), \tag{34}$$

obtained by looking at the response at the time t to an external field acting in the interval $(0,t_w)$

(2) The zero-field-cooled (ZFC) magnetization,

$$\chi(t,t_w,t_0,t_{sc},t_{eq})=\mu(t,t_2=t,t_1=t_w,t_0,t_{sc},t_{eq}), \tag{35}$$

obtained by looking at the response at the time t when the field acts in the interval (t_w,t).

Both these quantities do have shortcomings. For TRM the problem is evident. The integration starts at $t_1=0$, so preasymptotic contributions are always included. The dependence on t_{sc} cannot be neglected and this turns out to make it particularly hard to extract the asymptotic behavior in the cases of interest.

With ZFC magnetization there is no such problem. Taking $t_w\gg t_{sc}$, and neglecting t_{sc} thereafter, one can be confident to be in the asymptotic region where scaling holds. So, using (10) with $f(x,y)$ of the general form Eq. (20) and considering the case with $\epsilon=0$, one has

$$\chi_{ag}(t,t_w,t_0)=t_w^{-a}F(t/t_w,t_0/t_w) \tag{36}$$

with

$$F(x,y)=x^{-a}\int_{1/x}^{1}dz\frac{z^{\beta+\alpha-(a+1)}}{(1-z+y/x)^{\alpha}}. \tag{37}$$

The first observation is that if one seeks to determine a from Eq. (36) by looking at the behavior of χ_{ag} as t_w is varied and $x=t/t_w$ is kept fixed, one must be aware that the t_w dependence coming from t_0/t_w may play a role. In other words, $y=t_0/t_w$ may act as a dangerous irrelevant variable. Namely, defining the exponent a_χ by

$$\chi_{ag}(t,t_w)\sim t_w^{-a_\chi}\hat{\chi}(x), \tag{38}$$

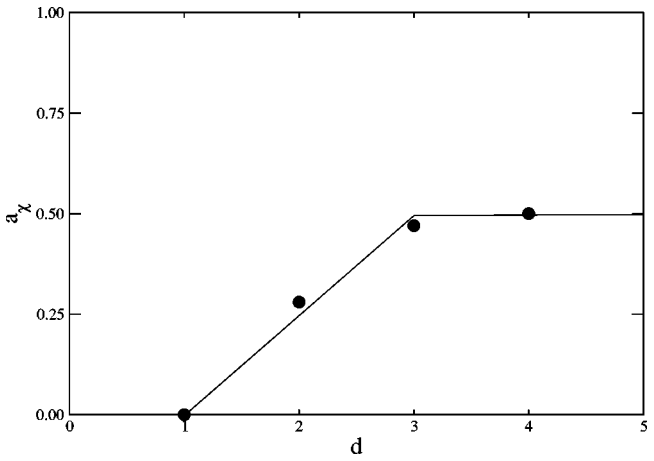

FIG. 1. Exponent a_χ in the Ising model at various dimensionalities. The continuous line represents Eq. (41), while the dots are the values from the exact solution of the model at $d=1$ and from simulations with $d=2,3,4$.

there may be a difference between a in Eq. (36) and a_χ in Eq. (38). This depends on whether the integral in Eq. (37) diverges or not at the upper limit of integration as $y\to 0$. This, in turn, depends on the value of α. The second observation is that α can be extracted from the large x behavior of $F(x,y)$, as we shall see in the following. Instead, the task of extracting β from Eq. (37) remains exceedingly complicated.

A. The exponents a and a_χ

The possibility that a_χ might not be identifiable with a, due to the presence of $y=t_0/t_w$, can be checked explicitly in the large-N model [16] and in the GAF approximation [5,13], where ZFC magnetization can be calculated with arbitrary d. In both cases there is a value d_χ of the dimensionality such that y is dangerous irrelevant above d_χ. This implies that a_χ coincides with a for $d<d_\chi$ and is given by Eqs. (16) and (18). Instead, a_χ is different from a and is given by

$$a_\chi=\delta \tag{39}$$

for $d>d_\chi$ with δ given by Eq. (25), which is independent of dimensionality. Logarithmic corrections appear at $d=d_\chi$, much in the same way as at the upper critical dimensionality in ordinary critical phenomena. The relation between a_χ and a in these two models is given by

$$a_\chi=\begin{cases} a & \text{for} \quad d<d_\chi \\ \delta & \text{with logarithmic corrections for} \quad d=d_\chi \\ \delta & \text{for} \quad d>d_\chi \end{cases} \tag{40}$$

with $\delta=1$ and $d_\chi=4$ in the large-N model and with $\delta=1/2$ and $d_\chi=2$ in the GAF approximation. We emphasize that in these two solvable cases, Eq. (39) holds only for $d>d_\chi$ where $a_\chi\neq a$.

Next, from extensive numerical simulations [17,5,18] of the Glauber-Ising model with $d=2,3,4$ we have measured a_χ obtaining data which are fairly well consistent (Fig. 1) with the phenomenological formula

$$a_\chi=\begin{cases} (d-1)/4 & \text{for} \quad d<3 \\ 1/2 & \text{with logarithmic corrections for} \quad d=3 \\ 1/2 & \text{for} \quad d>3. \end{cases} \tag{41}$$

Since in the scalar case $\delta=1/2$, it is evident that pattern (40) is followed also in the Ising model with $d_\chi=3$.

We may, then, conclude that in all cases—exact, approximate, and numerical—a_χ is given by Eq. (40) and that, therefore, the exponent a obeys the general formula

$$a=\delta\frac{d-d_L}{d_\chi-d_L}, \tag{42}$$

where d_L is the dimensionality where $a=0$. According to this picture, the distinction among the different systems comes through the values of δ, d_χ, and d_L (see Table I).

TABLE I. Values of δ, d_L, and d_χ in the different models.

	Ising	GAF	$N=\infty$
δ	1/2	1/2	1
d_L	1	1	2
d_χ	3	2	4

In this respect, notice that for $N=1$ both from simulations and from GAF one has $\delta=1/2$ and $d_L=1$, while there is a discrepancy between $d_\chi=3$ and $d_\chi=2$. However, this is not worrisome. As explained in Ref. [5], the dimensionality dependence of a_χ below d_χ takes place because d_χ is the dimensionality below which minimization of magnetic energy competes effectively with minimization of surface tension in driving interface motion. Therefore, the balance of these two mechanisms is very sensitive to the treatment of surface tension and it should not come as a surprise that from an uncontrolled approximation, such as those of the GAF type, a value of d_χ which differs from the one observed in simulations is obtained. The shift from $d_\chi=3$ to $d_\chi=2$ means that in the GAF approximation surface tension is overestimated with respect to simulations.

B. The scaling function $\hat{\chi}(x)$ and the exponent a

Although the results described above [17,5,18] yield unequivocally $d_\chi=3$ for $N=1$, in order to treat this point most carefully, we have again investigated the behavior of $\chi_{ag}(t,t_w)$ with very accurate simulations of the Ising model with NCOP, $d=2,3,4$, and for different values of t_w in order to get data also on the scaling function $\hat{\chi}(x)$, which has not been studied previously.

First, let us illustrate the algorithm. There are several ways to isolate the aging contribution $\chi_{ag}(t,t_w)$. The most obvious is to compute the total $\chi(t,t_w)$ by simulating a quenched system and then to subtract from it the stationary part $\chi_{st}(t,t_w)$ obtained by simulation of a system in equilibrium at the final temperature of the quench. A different algo-

rithm was introduced by Derrida [27] regarding the stationary contribution as due to thermal fluctuations inside the bulk of domains and the aging part as produced from the interfaces. The next step is to isolate the spins belonging to an interface. In order to do this a parallel simulation is performed of two systems with different initial conditions. The first is prepared in equilibrium at the initial temperature and then is quenched to the final temperature T, while the second is in equilibrium at the final temperature T from the beginning. These two systems evolve with the same thermal history at the temperature T. At each time step spins that are flipped in the first system but not in the second are considered as interfacial and their response is assigned to the aging part.

These two methods are equivalent, but also numerically very inefficient. Let us refer to them as global methods. The reason for inefficiency is that in order to extract the response produced by the spins on the interfaces one has to simulate the whole lattice. Since the interface density decreases as $t^{-1/z}$ a huge amount of CPU time can be saved by an algorithm updating only the interfacial spins. We stress that a fast algorithm is crucial in order to have reliable results in a numerically hard problem such as this. Therefore, we have adopted a no-bulk-flip algorithm, where a list of interfacial spins is updated at each move following the criterion that a spin belongs to an interface if at least one of the nearest neighbors is not aligned. Only moves of the interfacial spins are allowed. We then take the response of this system as $\chi_{ag}(t,t_w)$.

In $d=1$ it can be shown [14] that the no-bulk-flip algorithm corresponds to taking the limit of an infinite ferromagnetic coupling ($J\to\infty$) in the Ising Hamiltonian and that this isolates exactly the aging part of the response function. With $d>1$ the $J\to\infty$ limit and the no-bulk-flip algorithm produce different dynamical evolutions and an argument analogous to the one in the $d=1$ case cannot be made. What happens is that the limit $J\to\infty$ does not isolate $\chi_{ag}(t,t_w)$ because, besides freezing spins in the bulk, it also freezes most of the interfacial spins. Notice that the no-bulk-flip dynamics does not obey detailed balance. This is simply due to the fact that bulk spins are frozen. However, this is not a serious problem since we already know that by restoring moves in the bulk detailed balance is recovered producing the stationary contribution in the response function, which we are not interested in.

We have performed the simulations with the no-bulk-flip algorithm, after checking that the results are consistent within 5% with those of the global algorithms. In practice, we measure the quantity

$$\chi_{ag}(t,t_w)=\frac{1}{\mathcal{N}h_0^2}\sum_{i=1}^{\mathcal{N}}\overline{\langle\sigma_i\rangle h_i}, \tag{43}$$

where h_i is a quenched configuration of an uncorrelated random field, which takes the values $\pm h_0$ with probability 1/2. The angular brackets stand for the average over thermal histories, generated with the no-bulk-flip algorithm, and the overbar denotes the average over random field configurations. Simulations have been performed at $T/T_C=0.66$ for all values of d (for the lattice size and the number of realizations see Table II). $\chi_{ag}(t,t_w)$ is measured in units J^{-1} and time in units of Monte Carlo steps. For each thermal history we have changed also the random field configuration.

TABLE II. Lattice size $\mathcal{N}$ and number of realizations in the computation of $\chi_{ag}(t,t_w)$ at different waiting times.

	$d=2$		$d=3$		$d=4$	
t_w	$\mathcal{N}$	Realiz.	$\mathcal{N}$	Realiz.	$\mathcal{N}$	Realiz.
25	1024^2	2000	100^3	1000	42^4	1600
50	1024^2	2000	150^3	1000	68^4	180
100	1024^2	2000	150^3	1500	68^4	75
250	1024^2	2300	150^3	2700		
500	1024^2	15 000				
1000	1024^2	17 000				
1750	1024^2	17 000				
2500	1024^2	6000				

First, we have obtained a_χ by plotting $\chi_{ag}(t,t_w)$ versus t_w, for fixed values of $x=t/t_w$. In the range of t_w explored there is excellent power law behavior. With $x=7$ we find (Fig. 2) $a_\chi=0.28$ for $d=2$, $a_\chi=0.47$ for $d=3$, and $a_\chi=0.50$ for $d=4$. These numbers reproduce the results obtained previously [17,5,18] confirming that a_χ in the Ising model obeys closely Eqs. (40) and (42) with $\delta=1/2$, $d_\chi=3$, and $d_L=1$ (see also Fig. 1). Furthermore, the observed behavior is with good accuracy independent of x, as is shown in the inset of Fig. 2. The presence of a logarithmic correction at $d=3$ is hard to establish from the data of Fig. 2 since we have only one decade in t_w. In Refs. [17,5] where $\chi_{ag}(t,t_w)$ was plotted against t for fixed t_w over four decades, the logarithmic behavior is accessible. Also, it should be mentioned that Eq. (41) is a phenomenological formula, so it is hard to say whether the measured value $a_\chi=0.47$ for $d=3$ is due to logarithmic corrections or to some other effect not captured by Eq. (41). In any case, the quality of the data

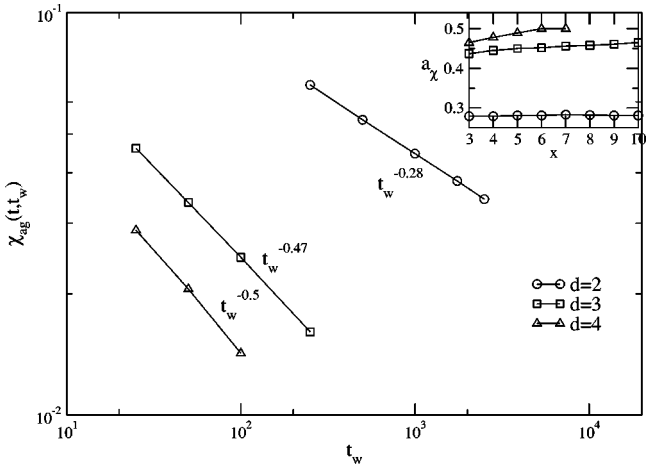

FIG. 2. $\chi_{ag}(t,t_w)$ vs t_w for fixed $x=t/t_w$. The slope yields a_χ. The plotted lines correspond to $x=7$. Values of a_χ for different values of x are depicted in the inset.

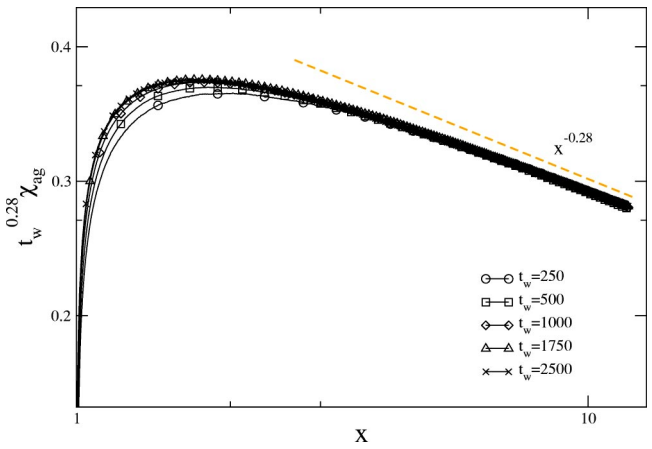

FIG. 3. Scaling function $\hat{\chi}(x)$ for the $d=2$ Ising model with $T/T_C=0.66$.

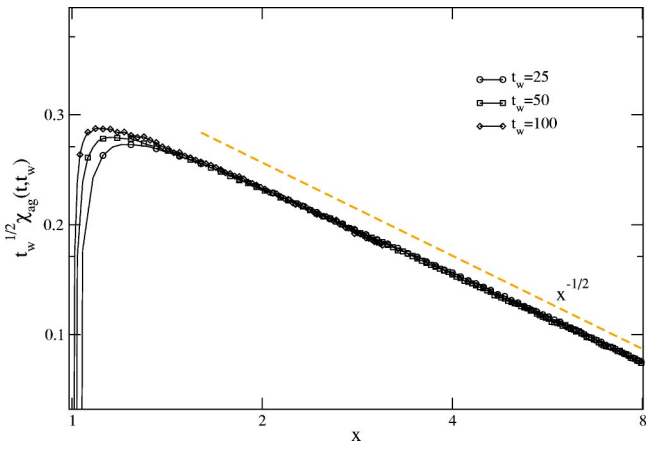

FIG. 5. Scaling function $\hat{\chi}(x)$ for the $d=4$ Ising model with $T/T_C=0.66$.

for $d=2$ allows to definitely rule out $a_\chi=0.5$, predicted by the qualitative argument referred to in the Introduction and to be discussed shortly.

Next, in order to investigate the scaling function $\hat{\chi}(x)$ in Eq. (38), notice that from Eqs. (36) and (37) follows the large x behavior

$$\hat{\chi}(x)\sim\begin{cases} x^{-a} & \text{for} \quad \alpha<1 \\ x^{-a}\ln x & \text{for} \quad \alpha=1 \\ x^{\alpha-a-1} & \text{for} \quad \alpha>1. \end{cases} \tag{44}$$

Using the values of a_χ from Fig. 2, we have plotted $t_w^{a_\chi}\chi_{ag}(t,t_w)$ versus $x=t/t_w$ for different values of t_w (Figs. 3–5).

Collapse of the data is obtained for x sufficiently large, where the scaling function decays with a power law and an exponent which coincides with a_χ. This is consistent with Eq. (44) only if $\alpha=a+1/2$ as in Eq. (26) and this rules out $\alpha=a+1$, which ought to apply according to the HPGL theory. Another way to see that $\alpha=a+1$ is untenable is that this would imply that $\hat{\chi}(x)$ goes to a constant for large x when $\alpha>1$. This, in turn, would lead to the unphysical conclusion that $\chi_{ag}(t,t_w)$ does not decay to zero for large t and fixed t_w when $d>d_\chi$. Therefore, we find that Eq. (26) holds for the Ising model not only for $d=1$, but also at higher dimensionality.

In conclusion, Eqs. (42) and (26) are our main results for a and α in the Ising model with d ranging from 1 to 4 and with Eq. (40) explaining how a is related to a_χ.

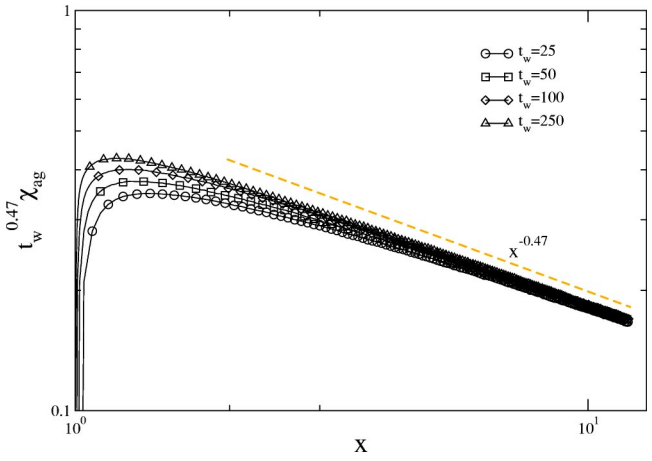

FIG. 4. Scaling function $\hat{\chi}(x)$ for the $d=3$ Ising model with $T/T_C=0.66$.

C. Qualitative conjecture on a_χ

We may now comment on the qualitative conjecture mentioned in the Introduction. Stating [10,7] that the aging contribution of ZFC magnetization ought to be proportional to the density of defects and assuming scaling, one finds

$$\chi_{ag}(t,t_w)\sim t_w^{-\delta}\hat{\chi}(t/t_w), \tag{45}$$

where δ is given by Eq. (25). This requires $a_\chi=\delta$ for all d contrary to the evidence presented above and summarized in Eq. (40), which restricts the validity of Eq. (39) to $d>d_\chi$. This makes a big difference, for instance, in the $d=2$ Ising model where from Eq. (40) $a_\chi=1/4$, while from Eq. (45) follows $a_\chi=1/2$. In order to understand why Eq. (45) breaks down below d_χ, let us go back to the behavior of $R_{ag}(t,s,t_0)$ in the short time regime. From Eq. (22) we may write

$$R_{ag}(t,s,t_0)\sim s^{-\delta}h(\tau,t_0), \tag{46}$$

where $h(\tau,t_0)$ is some function of the time difference. The meaning of this is that the response, due to an impulsive perturbation at the time s, is proportional to the density of defects at that instant of time with a proportionality factor containing the retardation effect. This does not hold anymore in the long time regime $\tau\gg s$. When the time interval τ is large with respect to s, multiple defect transits may have occurred through the observation site, spoiling form (46). Sticking to the short time regime, i.e., taking $t-t_w\ll t_w$ and using Eq. (46), from definition (35) follows

$$\chi_{ag}(t,t_w)\sim t_w^{-\delta}\chi_s(t-t_w), \tag{47}$$

where $\chi_s(t-t_w)$ is a function of the time difference, which in Refs. [5,17] we have identified with the ZFC magnetization associated with a single defect. Now, Eqs. (47) and (45) do require

$$\hat{\chi}(t/t_w) \sim \chi_s(t-t_w), \tag{48}$$

which can hold only if both functions are constant, and this is precisely the point. As we have explained in Refs. [5,17], $\chi_s(t-t_w)$ contains the cumulative effect on a single defect of the perturbation acting all along the time interval (t_w,t). This saturates rapidly to a constant when the defect degrees of freedom act paramagnetically and the underlying defect motion is uncorrelated with the external field. However, at dimensionalities low enough to reduce surface tension below the threshold where the external field may take part in driving defect motion, $\chi_s(t-t_w)$ acquires a nontrivial time dependence which renders $a_\chi \neq \delta$ for $d<d_\chi$. Finally, notice that in the framework of the qualitative conjecture with $a_\chi = \delta$ independent of dimensionality, there is no explanation for the exact $d=1$ result $a_\chi=0$. Instead, according to Eq. (41) this exact result, far from being an anomaly, is embedded as a limiting behavior in the smooth dimensionality dependence for $d<3$.

IV. TRM

Dealing with TRM, separation (33) gives $\rho(t,s) = \int_0^{t_w} R_{st}(t-s) + \int_0^{t_w} R_{ag}(t,s)$. Contrary to what happens for ZFC magnetization, where χ_{st} for long time saturates to a constant, here for the stationary contribution there are two possibilities: (i) if $R_{st}(t-s)$ decays exponentially $\rho_{st}(t-t_w)$ also decays exponentially or (ii) if $R_{st}(t-s)$ decays with a power law, like in the large-N model, $\rho_{st}(t-t_w)$ is subdominant with respect to $\rho_{ag}(t,t_w)$. In both cases we can neglect ρ_{st} and with it the distinction between ρ and ρ_{ag}.

As mentioned previously, TRM is affected by preasymptotic contributions which cannot be eliminated. This makes it quite difficult to establish if the asymptotic behavior has been reached in the simulations and ultimately to have a reliable estimate of a. In order to unravel what is the effect of the preasymptotic contributions on the scaling behavior of TRM, we have resorted as a guide to the solution of the large-N model (Sec. V). Here, we anticipate the results.

Assuming $t_w > t_{sc}$, in the large-N case there exists a dimensionality $d_\rho=4$ such that for $d<d_\rho$ TRM undergoes a crossover with a characteristic time t^*, which may also be much larger than t_{sc}. Introducing the effective exponent

$$a_{\rho,eff} = -\left.\frac{\partial \ln \rho(t,t_w,t^*)}{\partial \ln t_w}\right|_{t/t_w} \tag{49}$$

one finds

$$a_{\rho,eff} = \begin{cases} \lambda/z & \text{for} \quad t_w \ll t^* \\ a & \text{for} \quad t_w \gg t^*. \end{cases} \tag{50}$$

For $d=d_\rho$ there is a crossover from a pure power law to a power law with logarithmic correction

$$\rho(t,t_w,t^*) = \begin{cases} t_w^{-\lambda/z} E(t/t_w) & \text{for} \quad t_w \ll t^* \\ t_w^{-\lambda/z} \ln(t_w/t_{sc}) E(t/t_w) & \text{for} \quad t_w \gg t^*. \end{cases} \tag{51}$$

Finally, for $d>d_\rho$ one has the simple power law

$$\rho(t,t_w,t^*) = t_w^{-\lambda/z} E(t/t_w) \tag{52}$$

and for all values of d, in the time regime considered the scaling function obeys

$$E(x) \sim x^{-\lambda/z}. \tag{53}$$

Taking this pattern as a guide (with d_ρ, t^* and exponents model dependent) let us now turn to simulations of the Ising model. Analyzing data, the first thing to do is to check if a behavior of the type

$$\rho(t,t_w) \sim t_w^{-a_\rho} \hat{\rho}(t/t_w) \tag{54}$$

holds. If this is the case and if an exponent a_ρ can be meaningfully extracted, the next problem is relating a_ρ to a. According to the behavior found in the large-N model, the identification $a_\rho = a$ can be made only if $d<d_\rho$ and $t_w \gg t^*$. Numerical results for TRM in the Glauber-Ising model were first obtained by HPGL [8]. Plotting $\rho(t,t_w)$ against $x = t/t_w$ for different t_w in the range $t_w \in (25,250)$ for $d=2$ and $t_w \in (15,100)$ for $d=3$ they have obtained for a_ρ a result of the form

$$a_\rho = \begin{cases} 1/2 & \text{with logarithmic corrections for} \quad d=2 \\ 1/2 & \text{for} \quad d=3 \end{cases} \tag{55}$$

and they have made the identification $a=a_\rho$.

The next round of simulations was carried out by us [18] at the same temperatures and for the same system size as HPGL, but extending the range of t_w up to 2500 for $d=2$ and 250 for $d=3$. Performing a different data analysis, i.e., plotting $\rho(t,t_w)$ versus t_w for fixed $x=t/t_w$, we have found good agreement between the slope of the curves in the large t_w region, which in the log-log plot gives the effective exponent (49), and the known values of λ/z for the Ising model ($\lambda/z=5/8$ for $d=2$ and $\lambda/z=3/4$ for $d=3$). This is good evidence that in the scalar case TRM follows the crossover pattern obtained in the large-N model when $d<d_\rho$ and with a crossover time t^* larger than the maximum t_w that we have reached in the simulations. Furthermore, on the basis of our data, we have estimated that the largest t_w used by HPGL in Ref. [8] was not enough to enter the scaling regime (i.e., they had always $t_w \leqslant t_{sc}$) and therefore the values of a_ρ they have obtained do not warrant any statement, neither on the asymptotic value of a_ρ nor on a. Our longer range of t_w seems to be barely sufficient to enter the preasymptotic region where $a_{\rho,eff}=\lambda/z$, suggesting that both $d=2$ and $d=3$ are smaller than d_ρ, whose value in the Ising model, so far, we do not know. Hence, in order to observe the asymptotic exponent one should go to much longer waiting times t_w.

TABLE III. Lattice size $\mathcal{N}$ and number of realizations in the computation of $\rho_{ag}(t,t_w)$ at different waiting times.

	$d=2$		$d=3$	
t_w	$\mathcal{N}$	Realiz.	$\mathcal{N}$	Realiz.
25	1024^2	2000	100^3	1500
50	1024^2	2000	150^3	2500
100	1024^2	2000	150^3	2500
250	1024^2	13 000	150^3	2500
500	1024^2	16 000	160^3	2500
1000	1024^2	18 000		
1750	1024^2	23 000		
2500	1024^2	13 000		
5000	2048^2	7000		

Henkel and Pleimling [28] have produced new simulations for $d=2$ extending the range of t_w up to 5000. Plotting $\rho(t,t_w)$ versus t_w for fixed x and adhering to the point of view that the TRM data are affected by a long crossover, they claim (i) to have succeeded in going past the crossover time reaching the asymptotic region and (ii) to have found that Eq. (55) is verified. The objection to this claim is that in $d=2$ one has $\lambda/z=5/8>1/2>a_\chi=1/4$. Therefore, even if a decrease of the slope from a number close to $\lambda/z=0.625$ toward 0.5 is observed over a narrow time window, there is no way to decide whether the true asymptotic regime has been reached or the slope might still keep on decreasing, by going further with t_w, until reaching asymptotics at 0.25.

In other words, the new simulations in Ref. [28] leave the issue undecided and yet longer simulations are needed. Despite that, by now, there is sufficient evidence that TRM is not the most efficient and reliable way to get to the exponent a, we have undertaken simulations with t_w up to 5000 for $d=2$ and 500 for $d=3$ (for the lattice size and number of realizations see Table III).

The double logarithmic plot of $\rho(t,t_w)$ versus t_w for fixed x shows (Fig. 6) that a power law behavior, possibly, sets in only in the region of the largest t_w reached. Taking the slope in this region as a measure of $a_{eff,\rho}$ we find values (inset of Fig. 6) which lie above 0.5 for all x and that are just below $\lambda/z=0.625$ for $d=2$ and $\lambda/z=0.75$ for $d=3$. Hence, although we have reached the same maximum value of t_w as in Ref. [28] for $d=2$ and we have gone much farther for $d=3$, we may state that no evidence of asymptotic behavior with $a_\rho=1/2$ is found. Rather, the combination of the $d=2$ and $d=3$ data in Fig. 6 shows unequivocally that, at best, only the onset of the scaling region is entered where $a_{\rho,eff}$ is about to take the preasymptotic value λ/z, confirming the picture obtained in our previous work [18].

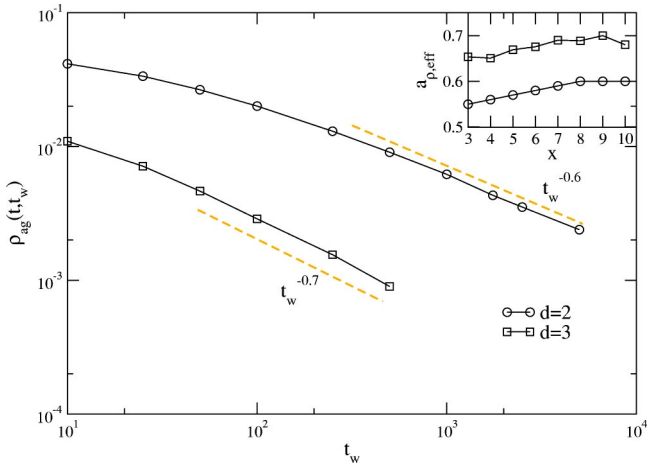

FIG. 6. $\rho_{ag}(t,t_w)$ vs t_w for fixed $x=7$. The slopes in the large t_w region yielding $a_{\rho,eff}$ for different values of x are depicted in the inset.

In summary, we have accumulated sufficient numerical evidence to establish that TRM data fit in the general pattern of behavior obtained from the solution of the large-N model, with $d_\rho>3$ and a value of t^* which is greater than the largest t_w reached so far. Therefore, since asymptotics has not been reached, no statement on a can be made from the present knowledge of TRM.

Finally, let us make a comment on the quotation in Refs. [8,29,30] of the analytical solution of the GAF approximation by Berthier *et al.* [13] as a support to the claim that a is given by Eq. (55). In fact, here is where is most evident the type of confusion that can arise by not being careful about which exponent one is talking about. In their computation Berthier *et al.* find $a_\chi=1/2$ for $d\geqslant 2$ with logarithmic correction at $d=2$, as in Eq. (55) which, however, is meant for a. What one should have clear in mind is that they compute an a_χ for $d\geqslant d_\chi$, i.e., right where $a_\chi\neq a$. This can be checked recalling that in the GAF approximation a is given by Eq. (18) and that $d_\chi=2$. Hence, for $d=2$ the logarithmic correction belongs to a_χ and not to a. For $d=3$ it is a_χ that takes the value 1/2, while from Eq. (18) follows $a=1$. So, the results of Berthier *et al.* certainly cannot be quoted if one wants to identify with a an exponent obeying Eq. (55).

V. TRM AND ZFC MAGNETIZATION IN THE LARGE-N MODEL

In this section we study in detail the large-N model [16,31] as a useful example which gives the complete picture of what happens when looking at the different response functions introduced above.

Consider a system with vector order parameter $\vec{\phi}(\vec{x})=(\phi_1(\vec{x}),\ldots,\phi_N(\vec{x}))$ and Hamiltonian of the Ginzburg-Landau form

$$\mathcal{H}[\vec{\phi}]=\int d^dx\left[\frac{1}{2}(\nabla\vec{\phi})^2+\frac{r}{2}\vec{\phi}^2+\frac{g}{4N}(\vec{\phi}^2)^2\right], \qquad (56)$$

where $r<0$, $g>0$. In the large-N limit the equation of motion for the generic component of the order parameter in Fourier space is given by [16]

$$\frac{\partial\phi(\vec{k},t)}{\partial t}=-[k^2+I(t)]\phi(\vec{k},t)+\eta(\vec{k},t), \qquad (57)$$

where $\eta(\vec{k},t)$ is a Gaussian white noise with expectations

$$\langle \vec{\eta}(\vec{k},t)\rangle = 0,$$

$$\langle \eta(\vec{k},t)\,\eta(\vec{k}',t')\rangle = 2T(2\pi)^d \delta(\vec{k}+\vec{k}')\,\delta(t-t'). \quad (58)$$

T is the temperature of the quench and the function of time

$$I(t) = r + g\langle \phi^2(\vec{x},t)\rangle \quad (59)$$

must be determined self-consistently, with the average on the right hand side taken both over thermal noise and initial conditions. The formal solution of Eq. (57) is given by

$$\phi(\vec{k},t) = R(\vec{k},t,0)\,\phi_0(\vec{k}) + \int_0^t ds R(\vec{k},t,s)\,\eta(\vec{k},s), \quad (60)$$

where $R(\vec{k},t,s)$ is the response function

$$R(\vec{k},t,s) = \frac{Y(s)}{Y(t)} e^{-k^2(t-s)} \quad (61)$$

with $Y(t) = \exp[Q(t)]$ and $Q(t) = \int_0^t ds I(s)$. With an uncorrelated initial state at very high temperature the initial condition $\phi_0(\vec{k}) = \phi(\vec{k},t=0)$ can be taken to be Gaussianly distributed with expectations

$$\langle \phi_0(\vec{k})\rangle = 0,$$

$$\langle \phi_0(\vec{k})\,\phi_0(\vec{k}')\rangle = \Delta(2\pi)^d \delta(\vec{k}+\vec{k}'). \quad (62)$$

The actual solution is obtained once the function $Y(t)$ is determined. In order to do this notice that from the definition of $Y(t)$ follows

$$\frac{dY^2(t)}{dt} = 2[r + g\langle \phi^2(\vec{x},t)\rangle]Y^2(t). \quad (63)$$

Writing $\langle \phi^2(\vec{x},t)\rangle$ in terms of the structure factor

$$\langle \phi^2(\vec{x},t)\rangle = \int \frac{d^dk}{(2\pi)^d} C(\vec{k},t) e^{-k^2/\Lambda^2}, \quad (64)$$

where Λ is the momentum cutoff and using Eq. (60) to evaluate $\langle \phi(\vec{k},t)\,\phi(\vec{k}',t)\rangle = C(\vec{k},t)(2\pi)^d \delta(\vec{k}+\vec{k}')$ we obtain

$$C(\vec{k},t) = R^2(\vec{k},t,0)\Delta + 2T\int_0^t ds R^2(\vec{k},t,s). \quad (65)$$

Then, inserting Eq. (64) into Eq. (63), we obtain the integro-differential equation

$$\frac{dY^2(t)}{dt} = 2rY^2(t) + 2g\Delta f\left(t + \frac{1}{2\Lambda^2}\right) + 4gT\int_0^t ds f\left(t - s + \frac{1}{2\Lambda^2}\right) Y^2(s), \quad (66)$$

where $f(x) \equiv \int d^dk/(2\pi)^d e^{-2k^2x} = (8\pi x)^{-d/2}$. After solving this equation, the response function is given by

$$R(t,s,t_0) = \int \frac{d^dk}{(2\pi)^d} R(\vec{k},t,s) e^{-k^2/\Lambda^2} = (4\pi)^{-d/2} \frac{Y(s)}{Y(t)} (t-s+t_0)^{-d/2}, \quad (67)$$

where $t_0 = 1/(2\Lambda^2)$.

Let us now come to the identification of the general structure of Eq. (5). Since in the stationary regime $Y(t)$ is time independent, we immediately obtain

$$R_{st}(t-s,t_0) = (4\pi)^{-d/2}(t-s+t_0)^{-d/2} \quad (68)$$

and

$$R_{ag}(t,s,t_0) = (4\pi)^{-d/2}\left[\frac{Y(s)}{Y(t)} - 1\right](t-s+t_0)^{-d/2}. \quad (69)$$

Notice that $R_{st}(t-s,t_0)$ is temperature independent, implying that there is a stationary response also at $T=0$. This holds for soft spins, while for Ising spins there is no stationary response at $T=0$.

Next, in order to investigate the scaling properties we must first learn about the time dependence of $Y(t)$. We do this in the $T=0$ case, since quenches below the critical point are controlled by the $T=0$ fixed point [2]. Making the ansatz $Y(t) = At^{-\omega}$ from Eq. (66) one gets

$$A\omega t^{-(2\omega+1)} = rAt^{-2\omega} + \frac{2g\Delta}{(8\pi)^{d/2}}(t+t_0)^{-d/2} \quad (70)$$

and assuming that the left hand side is negligible one finds $\omega = d/4$ with $A = (8\pi)^{-d/2}\Delta/M_0^2$, where $M_0 = \sqrt{-r/g}$ is the zero temperature magnetization. This is consistent if, in addition to $t \gg t_0$, one has also

$$t \gg t_{sc} = -d/(4r), \quad (71)$$

where the characteristic time t_{sc} sets the time scale over which the three terms in Eq. (70) are all of the same order of magnitude. Therefore, t_{sc} is the characteristic time separating the early from the late stage.

The above described behavior of $Y(t)$ is illustrated in Fig. 7 displaying the numerical solution of Eq. (66) for different values of r. In all numerical computations we will take $\Delta = 1$, $T=0$, and time is measured in units t_0. The onset of the scaling behavior is sharp and we have identified t_{sc} with the time where the power law begins (inset of Fig. 7). Then, for $s,t > t_{sc}$ from Eqs. (67) and (69) we have

$$R(t,s,t_0) = s^{-(1+a)}\tilde{f}(t/s, t_0/s) \quad (72)$$

with

$$\tilde{f}(x,y) = (4\pi)^{-d/2} x^{\omega}(x-1+y)^{-(1+a)}, \quad (73)$$

where

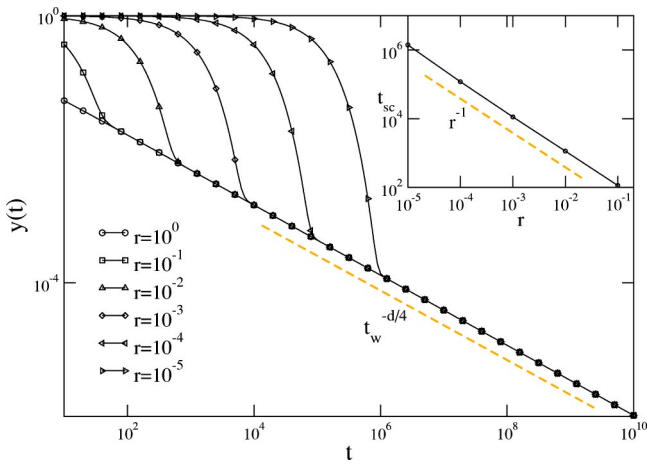

FIG. 7. $y(t)$ for different values of r and $T=0$. t_{sc} is estimated at the onset of the power law behavior and plotted against r in the inset.

$$a=(d-2)/2. \tag{74}$$

as in Eq. (16).

The connection between ω and λ/z can be established from the autocorrelation function. Keeping on considering $T=0$, from $C(\vec{k},t,s)=R(\vec{k},t,0)R(\vec{k},s,0)\Delta$ follows

$$C(t,s,t_0)=\int \frac{d^dk}{(2\pi)^d}C(\vec{k},t,s)e^{-k^2/\Lambda^2} \tag{75}$$

$$=(4\pi)^{-d/2}\Delta s^{2\omega-(1+a)}(t/s)^{\omega} \times[t/s+1+t_0/s]^{-(1+a)}. \tag{76}$$

The requirement $\lim_{t\to\infty}C(t,t)=M_0^2$ implies

$$2\omega=1+a \tag{77}$$

and comparing Eq. (76) with Eq. (5) we find

$$\omega=\lambda/z. \tag{78}$$

Hence, in the large-N model, λ and a are not independent exponents, since from Eqs. (77) and (78) follows

$$\lambda=1+a. \tag{79}$$

Nonetheless, for generality we shall keep on using the notation with two different exponents λ and a.

Finally, for the aging contribution (69) we may write

$$R_{ag}(t,s,t_0)=s^{-(1+a)}f(t/s,t_0/s) \tag{80}$$

with

$$f(x,y)=(4\pi)^{-d/2}(x^{\omega}-1)(x-1+y)^{-(1+a)} \tag{81}$$

and writing $\omega=1+a-\lambda/z$ Eq. (17) is recovered.

The above result shows that in the large-N model it is not only $R_{ag}(t,s)$ to scale, but also the full autoresponse function $R(t,s)$. This, obviously, means that $R_{st}(t-s)$ obeys scaling, as it can be checked immediately from Eq. (68) and this is a consequence of the fact that the whole low-temperature phase is critical.

A. TRM

We now explore the properties of the IRF in the large-N model. Let us begin from TRM. Since the explicit forms (68) and (80) with Eq. (81) show that $R_{st}(t-s,t_0)$ decays faster than $R_{ag}(t,s,t_0)$ with the time separation $t-s$, taking $t\gg t_w$ and using definitions (33) and (34) the stationary contribution to TRM can be neglected. Hence, in the following we will ignore the distinction between ρ and ρ_{ag}. Furthermore, taking $t_w>t_{sc}$ and dropping the dependence on t_0 we can write

$$\rho(t,t_w,t_{sc})=\frac{t^{-\lambda/z}}{(4\pi)^{d/2}A}\left[\int_0^{t_{sc}}dsY(s)+\int_{t_{sc}}^{t_w}dsY(s)\right], \tag{82}$$

where we have separated the preasymptotic from the asymptotic contribution in the integral. We shall see shortly that the first one plays a crucial role. Introducing the notation $B(t_{sc})=\int_0^{t_{sc}}dsY(s)$ and using $Y(s)=As^{-\lambda/z-(a+1)}$ in the second integral, we find

$$\rho(t,t_w,t_{sc})=t_w^{-\lambda/z}[K_0+K_1t_w^{\lambda/z-a}](t/t_w)^{-\lambda/z}, \tag{83}$$

where

$$K_0=(4\pi)^{-d/2}\left[\frac{B(t_{sc})}{A}-\frac{t_{sc}^{\lambda/z-a}}{(\lambda/z-a)}\right] \tag{84}$$

and

$$K_1=\frac{1}{(4\pi)^{d/2}(\lambda/z-a)}. \tag{85}$$

Equation (83) is the main result from which follows the nontrivial dependence of a_ρ on dimensionality. Notice that all the dependence on the preasymptotic behavior is collected in K_0 and the very presence of this nonvanishing term entails that the asymptotic power governing TRM is either λ/z or a according to the sign of $(\lambda/z-a)$. Therefore, writing $\lambda/z-a=(d_\rho-d)/d_\rho$ with $d_\rho=4$ we have a crossover for $d<d_\rho$, logarithmic corrections for $d=d_\rho$, and a correction to scaling for $d>d_\rho$.

Introducing the characteristic time

$$t^*=\left(\frac{K_0}{|K_1|}\right)^{1/[\lambda/(z-a)]}, \tag{86}$$

Eq. (83) for $d\neq d_\rho$ can be rewritten as

$$\rho(t,t_w,t^*)=t_w^{-\lambda/z}\tilde{E}(t/t_w,t^*/t_w) \tag{87}$$

with

$$\tilde{E}(x,y)=K_0[1\pm y^{\lambda/z-a}]x^{-\lambda/z}, \tag{88}$$

where the + and − signs apply to $d<d_\rho$ and $d>d_\rho$, respectively. In the first case the crossover time t^* is given by (Appendix)

$$t^*/t_{sc} \sim t_{sc}^{d/(4-d)} \tag{89}$$

showing that t^* is a new time scale which can become much larger than t_{sc}. Instead, in the second case from Eq. (86) follows (Appendix)

$$t^*/t_{sc} < 1 \tag{90}$$

implying $t_w/t^* > 1$ for any $t_w > t_{sc}$. Finally, for $d=d_\rho$ from Eq. (83) we have

$$\rho(t,t_w,t^*,t_{sc}) = (4\pi)^{-d/2} t_w^{-\lambda/z} \left[1 + \frac{\ln(t_w/t_{sc})}{\ln(t^*/t_{sc})}\right] \ln(t^*/t_{sc}) \times (t/t_w)^{-\lambda/z}, \tag{91}$$

where t^* is given by

$$t^*/t_{sc} = e^{Ct_{sc}} \tag{92}$$

and C is a constant (Appendix).

Therefore, as anticipated in Sec. IV, the scaling properties of TRM exhibit the following dimensionality dependence

$d<d_\rho$. There is a crossover with the effective exponent

$$a_{\rho,eff} = -\left.\frac{\partial \ln \rho(t,t_w,t^*)}{\partial \ln t_w}\right|_{t/t_w} = \lambda/z - \left[\frac{(t_w/t^*)^{\lambda/z-a}}{1+(t_w/t^*)^{\lambda/z-a}}\right] \times (\lambda/z - a) \tag{93}$$

yielding

$$a_{\rho,eff} = \begin{cases} \lambda/z & \text{for} \quad t_w \ll t^* \\ a & \text{for} \quad t_w \gg t^*. \end{cases} \tag{94}$$

$d=d_\rho$. The crossover involves a logarithmic correction

$$\rho(t,t_w,t^*) = \begin{cases} t_w^{-\lambda/z} E(t/t_w) & \text{for} \quad t_w \ll t^* \\ t_w^{-\lambda/z} \log(t_w/t_{sc}) E(t/t_w) & \text{for} \quad t_w \gg t^*. \end{cases} \tag{95}$$

$d>d_\rho$. There is a pure power law for all $t_w > t_{sc}$,

$$\rho(t,t_w,t^*) = t_w^{-\lambda/z} E(t/t_w) \tag{96}$$

with

$$E(x) \sim x^{-\lambda/z}. \tag{97}$$

In the end, in the large-N model the relation between a and the exponent a_ρ appearing in Eq. (54) is given by

$$a_\rho = \begin{cases} a & \text{for} \quad d<d_\rho \\ \lambda/z & \text{with logarithmic corrections for} \quad d=d_\rho \\ \lambda/z & \text{for} \quad d>d_\rho, \end{cases} \tag{98}$$

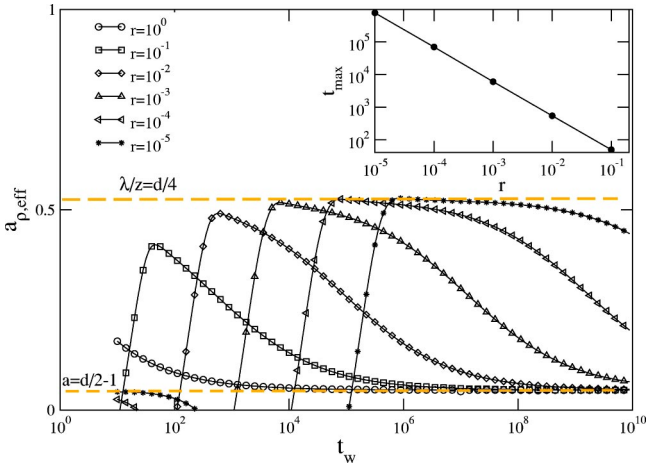

FIG. 8. Effective exponent $a_{\rho,eff}$ in the large-N model vs t_w for different values of r with $x=20$, $d=2.1$, and $T=0$. The value of t_w at the maximum corresponds to t_{sc} as shown in the inset.

where $d_\rho=4$.

In order to illustrate the behavior of TRM we have solved numerically for $\rho(t,t_w)$. In Fig. 8 we have plotted the effective exponent (93) versus t_w for different values of r (giving rise to different values of t_{sc}), with fixed $x=t/t_w=20$ and for $d=2.1<d_\rho$. The curves show quite clearly three different regimes: the early regime to the left of the peak followed by the intermediate regime going like $t_w^{-\lambda/z}$, whose size depends on t_{sc}, and eventually by the late stage regime going like t_w^{-a}. The value t_{max} of t_w at the peak can be identified with t_{sc} since it depends on r according to Eq. (71) (see inset of Fig. 8). For completeness we have plotted the same figure for $d=5>d_\rho$ (Fig. 9) which shows the existence only of the early regime followed immediately by the asymptotic regime with the exponent λ/z (without any crossover or intermediate scaling regime) according to Eq. (96).

B. ZFC magnetization

Taking $t_w > t_{sc}$ and using definitions (33), (68), and (69) we have

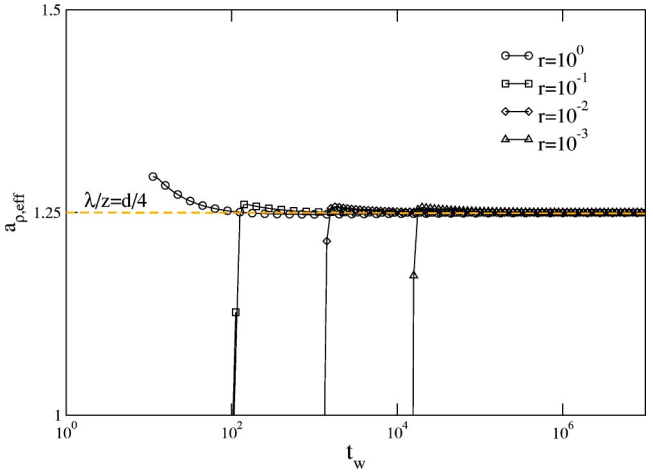

FIG. 9. Effective exponent $a_{\rho,eff}$ in the large-N model vs t_w for different values of r with $x=20$, $d=5$, and $T=0$.

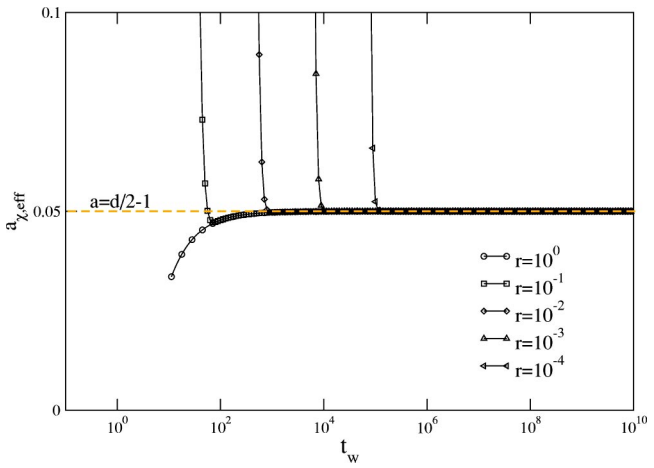

FIG. 10. Effective exponent $a_{\chi,eff}$ in the large-N model vs t_w for different values of r with $x=20$, $d=2.1$, and $T=0$.

$$\chi_{st}(t-t_w,t_0)=\frac{2t_0^{1-d/2}}{(4\pi)^{d/2}(d-2)}\{1-[(t-t_w)/t_0+1]^{-a}\} \tag{99}$$

and

$$\chi_{ag}(t,t_w,t_0)=t_w^{-a}F(t/t_w,t_0/t_w) \tag{100}$$

with

$$F(x,y)=(4\pi)^{-d/2}x^{-a}\int_{1/x}^{1}du(u^{\lambda/z-(1+a)}-1)$$
$$\times(1-u+y/x)^{-(1+a)}. \tag{101}$$

Therefore, in order to establish how χ_{ag} scales with t_w it is necessary to know how the scaling function $F(x,y)$ behaves for small y. As already pointed out, this depends on the behavior of the integral at the upper limit of integration, which is convergent (divergent) for $a<1$ ($a\geqslant 1$). Hence, from $1-a=(d_\chi-d)/2$ with $d_\chi=4$ follows

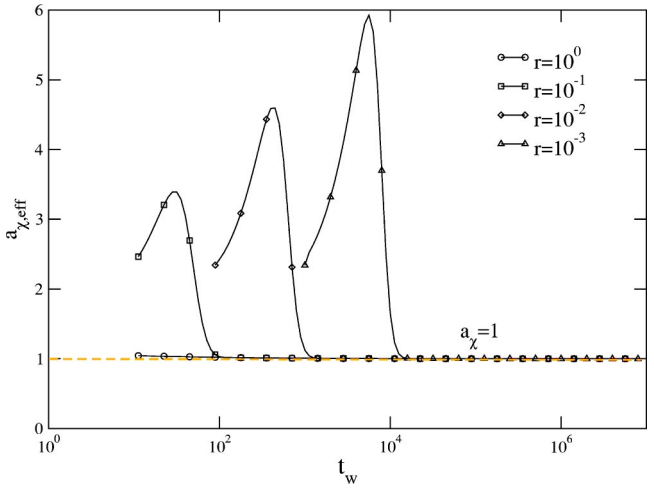

FIG. 11. Effective exponent $a_{\chi,eff}$ in the large-N model vs t_w for different values of r with $x=20$, $d=5$, and $T=0$.

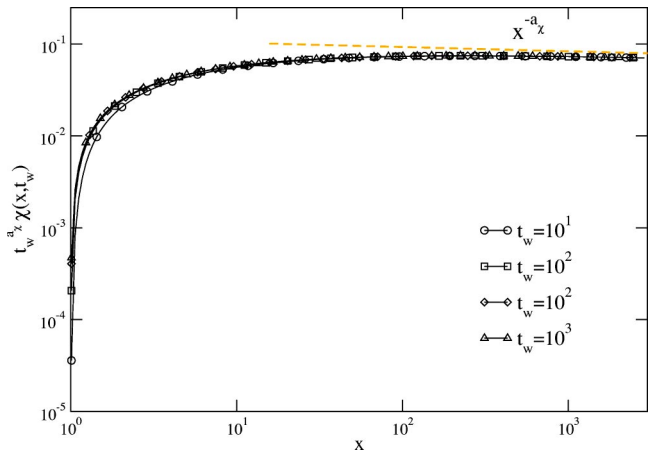

FIG. 12. Scaling function $\hat{\chi}(x)$ in the large-N model with $d=2.1$ and $T=0$. In this case $a_\chi=a=0.05$.

$$F(x,y)\sim\begin{cases}x^{-a} & \text{for} \quad d<d_\chi\\ x^{-a}\ln(x/y) & \text{for} \quad d=d_\chi\\ y^{1-a}/x & \text{for} \quad d>d_\chi.\end{cases} \tag{102}$$

Inserting into Eq. (100) and comparing with Eq. (38) we recover Eqs. (40) and (42). Finally, for large x we obtain the analogous form of Eq. (44),

$$\hat{\chi}(x)\sim\begin{cases}x^{-a} & \text{for} \quad d<d_\chi\\ x^{-a}\ln x & \text{for} \quad d=d_\chi\\ x^{-1} & \text{for} \quad d>d_\chi.\end{cases} \tag{103}$$

Notice that the separation of the stationary from the aging response function has played a crucial role. Had we used form (31) of HPGL in Eq. (101) we would have obtained a completely different behavior, with $d_\chi=2$ and in place of Eq. (40),

$$a_\chi=\begin{cases}a=d/2-1 & \text{for} \quad d<2\\ 0 & \text{with logarithmic corrections for} \quad d=2\\ 0 & \text{for} \quad d>2.\end{cases} \tag{104}$$

In order to illustrate the difference in the behaviors of TRM and ZFC magnetization we have solved numerically for $\chi_{ag}(t,t_w)$ and for the corresponding effective exponent $a_{\chi,eff}(t_w,x)$ (Figs. 10 and 11) with the same values of d and r used for TRM. These figures show that both above and below d_χ there is no crossover, but there is only the early regime followed abruptly by the asymptotic power law behavior, as for TRM above d_ρ (Fig. 9). Furthermore, we have depicted in Figs. 12 and 13 the scaling function $\hat{\chi}(x)$, obtained by plotting $t_w^{a_\chi}\chi_{ag}(t_w,x)$ versus x for different t_w, which obeys the power laws (103) for large x. These are the analogous forms of Figs. 3 and 5.

We can now summarize what we have learned from the large-N model about the connection between a_ρ, a_χ, and a. In this case the explicit solution (74) is available and a is a linearly increasing function of dimensionality vanishing at

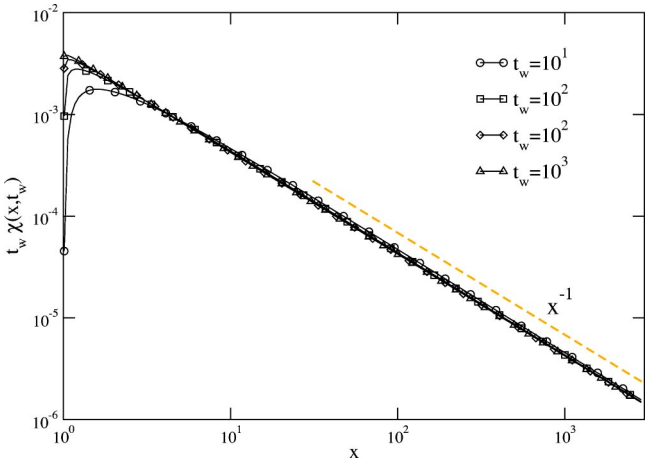

FIG. 13. Scaling function $\hat{\chi}(x)$ in the large-N model with $d=5$ and $T=0$. In this case $a_\chi=1$ and $a=1.5$.

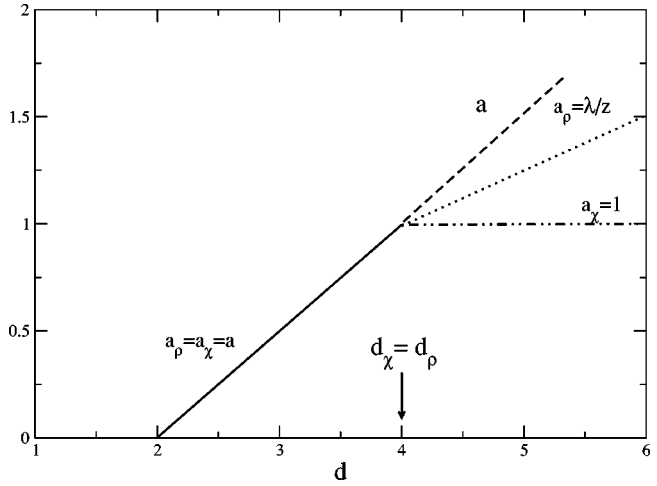

FIG. 14. Overview of the dimensionality dependence of the exponents a, a_χ, a_ρ in the large-N model.

$d_L=2$. The question is how much of this could have been inferred relying only on the information from TRM or ZFC. The answer is that both a_ρ and a_χ coincide with a below certain dimensionalities d_ρ and d_χ. At $d=d_\rho$ and $d=d_\chi$ there are logarithmic corrections, while above these dimensionalities a_ρ and a_χ are different from a and differ one from the other (Fig. 14). Although in the large-N model $d_\rho=d_\chi=4$, we have kept distinct notations because d_ρ, which is the dimensionality where $\lambda/z=a$, and d_χ the dimensionality where $a-1=0$, need not to coincide in general. In the large-N model they do coincide because of Eq. (79). Furthermore, even below d_ρ and d_χ, where $a_\rho=a_\chi=a$, there remains a considerable difference between TRM and ZFC in relation to the time scales (t^* and t_{sc}) over which these exponents are observable. Comparing Figs. 8 and 10 one can see at a glance that the difference between these time scales in certain conditions, here set by the value of r, can become huge and if working with TRM it may require an enormous t_w before reaching the asymptotic regime where a_ρ and a can be identified.

VI. CONCLUDING REMARKS AND OPEN PROBLEMS

In conclusion, we have shown that all existing analytical results and the numerical evidence coming from ZFC magnetization in the Ising model are consistent with an exponent a of form (42). The dimensionality independent behavior (39) predicted by the qualitative argument for a_χ holds only for $d>d_\chi$ where $a_\chi\neq a$. This is due to the presence of a dangerous irrelevant variable. Once this is taken into account, analytical and numerical results form a coherent picture and the issue can be considered as settled.

For what concerns Eq. (55), regarded in Refs. [8,28–30] as the exponent a in the Ising model, we have shown that it does not have any analytical foundation, because Ref. [13] contains a computation of a_χ. Furthermore, the numerical evidence, being based on TRM data, is inconclusive since the largest t_w reached so far are below the crossover time t^*. Therefore, t_w is still far from being well inside the asymptotic region as required for the TRM data to qualify as a challenge to those obtained from ZFC magnetization. There is no doubt that among all possible IRFs that one can employ to study the exponent a, TRM is the most unfavorable and the least reliable one, as abundantly explained in the previous sections.

For what concerns the scaling function $f(x,y)$, our ZFC data are consistent with an $f(x,y)$ in the Ising model of form (20) with the exponent $\alpha=a+1/2$ in place of $\alpha=a+1$, appearing in the HPGL theory. We have also shown that with the HPGL theory it is not possible to reproduce the short time behavior of $R_{ag}(t,s,t_0)$. Nonetheless, our knowledge of the scaling function $f(x,y)$ is still incomplete, since from ZFC data we cannot determine the exponent β.

After this survey of what can and what cannot be done with ZFC and TRM data, it seems clear that in order to study $R_{ag}(t,s,t_0)$ the right thing to do would be to use neither of them. Rather, one should use an IRF of the general form (32) with $t_1 \gg t_{sc}$ to eliminate the crossover affecting TRM and with $t_2<t$ in order to avoid the dangerous irrelevant variable in the ZFC magnetization. Namely, assuming form (20) of $f(x,y)$ and using Eq. (32) one should consider

$$\mu_{ag}(t,t_2,t_1,t_0)=t^{-a}\int_{t_1/t}^{t_2/t} dz \frac{z^{\beta+\alpha-1-a}}{(1-z+t_0/t)^\alpha}. \quad (105)$$

If $t_2<t$ and $t\gg t_0$, the dependence on t_0 can be neglected and the above equation can be used in two ways. Rewriting

$$\mu_{ag}(t,t_2,t_1)=t^{-a}\int_{x_1}^{x_2} dz \frac{z^{\beta+\alpha-1-a}}{(1-z)^\alpha} \quad (106)$$

and keeping $x_1=t_1/t$ and $x_2=t_2/t$ fixed, the exponent a can be measured. Next, for $t\gg t_2$ from Eq. (105) follows

$$\mu_{ag}(t,t_2,t_1)\sim t^{-a}\int_{t_1/t}^{t_2/t} dz z^{\beta+\alpha-1-a}\sim t^{-(\beta+\alpha)} \quad (107)$$

from which $\beta+\alpha$ can be measured, while α, as we have seen, can be extracted from $\hat{\chi}(x)$. We plan to pursue the investigation of this IRF in future work.

Finally, the results obtained in this paper open a number of interesting problems in the general theory of phase order-

ing. We stress that our results are phenomenological. In particular, we do not know why d_L and d_χ take the values they take. d_L seems to coincide with the ordinary lower critical dimensionality, but we do not know whether this is really so, or if it is just a coincidence. We can tell even less about the values taken by the upper dimensionality d_χ. We should note the failure of the GAF approximation to reproduce the correct dependence of a on d in the scalar case. In short, we have no theory for the observed behavior of the response function in phase-ordering kinetics.

ACKNOWLEDGMENT

This work was partially supported from MURST through Grant No. PRIN-2002.

APPENDIX

From definitions (84), (85), and (86) we have

$$t^* = \left[\frac{B(t_{sc})|\lambda/z - a|}{A} \pm t_{sc}^{\lambda/z - a} \right]^{1/(\lambda/z - a)} \tag{A1}$$

with the $+$ $(-)$ sign if $\lambda/z - a < (>) 0$, i.e if $d > (<) 4$. In order to estimate $B(t_{sc})$ we use the linear approximation

$$B(t_{sc}) = \int_0^{t_{sc}} e^{rs} = (e^{r t_{sc}} - 1)/r. \tag{A2}$$

Then, using $A = (8\pi)^{-d/2} \Delta / M_0^2$ and $t_{sc} = -d/4r$ we find

$$B(t_{sc})/A = C t_{sc} \tag{A3}$$

with

$$C = 4(8\pi)^{d/2}(1 - e^{-d/4}) M_0^2 / \Delta d \tag{A4}$$

and inserting into Eq. (A1) we get

$$t^*/t_{sc} = \left[\frac{(4-d)}{4} C t_{sc}^{d/4} \pm 1 \right]^{4/(4-d)}. \tag{A5}$$

For $d < 4$ the above equation must be taken with the minus sign. This requires $t_{sc} > [C(4-d)/4]^{-4/d}$ or $4|r|/d < [C(4-d)/4]^{4/d}$. To lift this restriction on the value of r one must do better than the linear approximation in the estimate of $B(t_{sc})$. Taking t_{sc} large enough, Eq. (89) is obtained.

If $d > 4$, instead, from Eq. (A5) follows $t^* < t_{sc}$ justifying Eq. (96).

Finally, for $d = 4$ from Eq. (83) we get

$$\rho(t, t_w, t^*, t_{sc}) = t_w^{-\lambda/z} \left[\frac{B(t_{sc})}{A} + \ln(t_w/t_{sc}) \right] \times (4\pi)^{-d/2} (t/t_w)^{-\lambda/z} \tag{A6}$$

and defining t^* by

$$\ln(t^*/t_{sc}) = B(t_{sc})/A, \tag{A7}$$

Eqs. (91) and (92) are recovered after using Eq. (A3).

[1] For a recent review, see L.F. Cugliandolo, e-print cond-mat/0210312.
[2] For a review, see A.J. Bray, Adv. Phys. **43**, 357 (1994).
[3] See, for instance, J.P. Bouchaud, L.F. Cugliandolo, J. Kurchan, and M. Mézard, in *Spin Glasses and Random Fields*, edited by A.P. Young (World Scientific, Singapore, 1997).
[4] For a recent review, see A. Crisanti and F. Ritort, J. Phys. A **36**, R181 (2003).
[5] F. Corberi, E. Lippiello, and M. Zannetti, Eur. Phys. J. B **24**, 359 (2001).
[6] N. Fusco and M. Zannetti, Phys. Rev. E **66**, 066113 (2002).
[7] S. Franz, M. Mézard, G. Parisi and L. Peliti, Phys. Rev. Lett. **81**, 1758 (1998); J. Stat. Phys. **97**, 459 (1999).
[8] M. Henkel, M. Pleimling, C. Godrèche, and J.M. Luck, Phys. Rev. Lett. **87**, 265701 (2001).
[9] M. Henkel, Nucl. Phys. B **641**, 405 (2002).
[10] A. Barrat, Phys. Rev. E **57**, 3629 (1998).
[11] G. Parisi, F. Ricci-Terzenghi, and J.J. Ruiz-Lorenzo, Eur. Phys. J. B **11**, 317 (1999).
[12] A. Montanari and F. Ricci-Terzenghi, e-print cond-mat/0305044.
[13] L. Berthier, J.L. Barrat, and J. Kurchan, Eur. Phys. J. B **11**, 635 (1999).
[14] E. Lippiello and M. Zannetti, Phys. Rev. E **61**, 3369 (2000).
[15] C. Godrèche and J.M. Luck, J. Phys. A **33**, 1151 (2000).
[16] F. Corberi, E. Lippiello, and M. Zannetti, Phys. Rev. E **65**, 046136 (2002).
[17] F. Corberi, E. Lippiello, and M. Zannetti, Phys. Rev. E **63**, 061506 (2001).
[18] F. Corberi, E. Lippiello and M. Zannetti, Phys. Rev. Lett. **90**, 099601 (2003).
[19] A.J. Bray, J. Phys. A **22**, L67 (1989).
[20] A. Prados, J.J. Brey, and B. Sànchez-Rey, Europhys. Lett. **40**, 13 (1997).
[21] F. Corberi, C. Castellano, E. Lippiello, and M. Zannetti, Phys. Rev. E **65**, 066114 (2002).
[22] For reasons different from ours, the distinction between systems with short (class S) and long (class L) range correlations has been made by M. Henkel, M. Paessens, and M. Pleimling, e-print cond-mat/0211583. These authors, contrary to us, regard the $d = 1$ Ising model as belonging to class L.
[23] C. Godrèche and J.M. Luck, J. Phys. A **33**, 9141 (2000).
[24] L.F. Cugliandolo and D.S. Dean, J. Phys. A **28**, 4213 (1995).
[25] W. Zippold, R. Kűhn, and H. Horner, Eur. Phys. J. B **13**, 531 (2000).
[26] P. Calabrese and A. Gambassi, Phys. Rev. E **66**, 066101 (2002); **67**, 036111 (2002).
[27] B. Derrida, Phys. Rev. E **55**, 3705 (1997).
[28] M. Henkel and M. Pleimling, Phys. Rev. Lett. **90**, 099602 (2003).
[29] M. Henkel, M. Paessens, and M. Pleimling, Europhys. Lett. **62**, 664 (2003).
[30] M. Henkel and M. Pleimling, e-print cond-mat/0302482.
[31] G.F. Mazenko and M. Zannetti, Phys. Rev. Lett. **53**, 2106 (1984); Phys. Rev. B **32**, 4565 (1985); A. Coniglio, P. Ruggiero, and M. Zannetti, Phys. Rev. E **50**, 1046 (1994).